PNAS RESEARCH ARTICLE | BIOCHEMISTRY

eIF2Bδ blocks the integrated stress response and maintains eIF2B activity and cancer metastasis by overexpression in breast cancer stem cells

Malavika Gupta[a,1], Beth A. Walters[a,2], Olga Katsara[a], Karol Granados Blanco[a], Phillip A. Geter[a,3], and Robert J. Schneider[a,b,4]

Edited by Joseph Puglisi, Stanford University School of Medicine, Stanford, CA; received May 6, 2022; accepted March 8, 2023

Breast cancer (BC) metastasis involves cancer stem cells (CSCs) and their regulation by micro-RNAs (miRs), but miR targeting of the translation machinery in CSCs is poorly explored. We therefore screened miR expression levels in a range of BC cell lines, comparing non-CSCs to CSCs, and focused on miRs that target translation and protein synthesis factors. We describe a unique translation regulatory axis enacted by reduced expression of miR-183 in breast CSCs, which we show targets the eIF2Bδ subunit of guanine nucleotide exchange factor eIF2B, a regulator of protein synthesis and the integrated stress response (ISR) pathway. We report that reduced expression of miR-183 greatly increases eIF2Bδ protein levels, preventing strong induction of the ISR and eIF2α phosphorylation, by preferential interaction with P-eIF2α. eIF2Bδ overexpression is essential for BC cell invasion, metastasis, maintenance of metastases, and breast CSC expansion in animal models. Increased expression of eIF2Bδ, a site of action of the drug ISRIB that also prevents ISR signaling, is essential for breast CSC maintenance and metastatic capacity.

breast cancer | metastasis | translational regulation | integrated stress response | unfolded protein response

Significance

Cancer stem cells (CSCs) are responsible for the metastatic activity of many cancer types, but must withstand physiological stresses that inhibit protein synthesis. We discovered that breast CSCs are deficient in microRNA-183 compared to breast cancer cells. MicroRNA-183 targets the delta subunit of translation factor eIF2B, a guanine exchange factor that controls protein synthesis during cell stress. This deficiency results in increased levels of eIF2Bδ protein, which is essential for survival and metastasis of breast CSCs, for suppression of the integrated stress response (ISR), and maintenance of protein synthesis under physiological stress. Our findings identify a regulatory mechanism of the ISR and protein synthesis that is also essential for breast cancer metastasis.

Many solid tumors contain a small (1 to 2%) population of cancer stem cells (CSCs), which promote cancer cell invasion and metastasis, and are thought to arise from normal adult tissue stem cells that gained increased proliferation, renewal, and transformed phenotypes (1–3). CSCs can be defined functionally by their ability to proliferate nonadherently as spheroids, resistance to staining with permeable dyes known as a "side-population" by flow cytometry, increased tumor cell invasion, and migration and metastatic activity in cell culture and animal models, among other parameters (4). Biomarkers including $CD44^{high}/CD24^{low}$, and high aldehyde dehydrogenase activity ($Aldh^{+}$), determined by Aldefluor staining, also define CSCs (4).

Given that CSCs survive as nonadherent cells with high migratory capacity and are under significant physiological stress, it is likely they have developed novel mechanisms of translational regulation which have not been well studied, including that by microRNAs (miRs). CSCs and non-CSCs are differentially controlled by the miRs they express (5–7). miRs bind to messenger RNAs (mRNAs) through a short seed sequence, often in the 3′ untranslated region (UTR) but also in the coding region and the 5′UTR. Differential miR expression in CSCs promotes an invasive and metastatic phenotype of malignant cancers (8–10). Notably, while increased expression of certain miRs promotes CSC viability and invasive/metastatic properties, loss of expression of other miRs can also promote key CSC properties, including the epithelial-to-mesenchymal transition (EMT), cell migration, metastatic capacity, and chemoresistance (5–7).

Surprisingly, few miRs have been identified that target protein synthesis factors. The identified miRs are limited to miR-138-5p that targets 4E-BP1 (11), miR-768-3p and miR-15a-5p that target eIF4E (12, 13), and the miR-322/miR-503 cluster that modestly targets eIF4GI, eIF4B, and eIF3m (14, 15). To date, no translation factor targeting miRs has been identified in CSCs (5).

Translation initiation involves 40S ribosome subunit scanning on mRNA, association with a 60S ribosome subunit at the initiation codon, hydrolysis of guanosine triphosphate (GTP) on eIF2, and release of eIF2-guanosine diphosphate (GDP) (16). For subsequent rounds of initiation to take place, the GDP on eIF2 must be replaced with GTP, which is carried out by guanine exchange factor (GEF) eIF2B. eIF2B-GDP to GTP exchange is a major control point in eukaryotic protein synthesis (16, 17). In response to a variety of cell stresses, any of the four protein kinases phosphorylate the eIF2α subunit at Ser-51, which raises its binding affinity for eIF2B, competitively inhibiting eIF2B GEF activity and impairing translation initiation (16, 17). Of the four kinases, protein kinase R-like

Author contributions: M.G., B.A.W., O.K., P.A.G., and R.J.S. designed research; M.G., B.A.W., O.K., K.G.B., and P.A.G. performed research; M.G., B.A.W., O.K., and K.G.B. contributed new reagents/analytic tools; M.G., B.A.W., O.K., and R.J.S. analyzed data; and M.G., B.A.W., and R.J.S. wrote the paper.

The authors declare no competing interest.

This article is a PNAS Direct Submission.

[1]Present address: Carecam International, Inc, Fairfield, NJ 07004.

[2]Present address: Ultragenyx Pharmaceuticals, Novato, CA 94949.

[3]Present address: Wunderman Thompson Health, New York, NY 10007.

[4]To whom correspondence may be addressed. Email: Robert.schneider@nyumc.org.

This article contains supporting information online at https://www.pnas.org/lookup/suppl/doi:10.1073/pnas.2207898120/-/DCSupplemental.

Published April 4, 2023.

endoplasmic reticulum (ER) kinase (PERK) is most involved in the integrated stress response (ISR) (16, 17). eIF2B GEF activity is the key site of translational regulation by the ISR pathway through eIF2α phosphorylation (18). eIF2B is a decameric protein complex comprised of two pentamers of regulatory (α, β, δ) and catalytic (γ, ε) protein subunits that carries out GEF activity (18–21). Studies have linked both increased and decreased activities of eIF2B to cellular transformation and cancer progression (22–24).

Here, we provide evidence for the regulation of a translation factor in breast CSCs by a miR. We show that increased expression of the eIF2Bδ subunit of eIF2B in breast CSCs is necessary for promotion and maintenance of metastatic activity of breast cancer (BC). The increase in eIF2Bδ in breast CSCs results from the reduced expression of miR-183. We show that increased expression of eIF2Bδ impairs activation of the ISR under stress by preferentially binding eIF2α-P, which is essential for promoting cancer cell migration, invasion, and metastasis, and is required for maintenance of the CSC population in animal models of BC.

Results and Discussion

Reduced miR-183 Levels in Breast CSCs Increase eIF2Bδ Expression. CSCs from nine representative BC cell lines, from immortalized to highly metastatic, were isolated by FACS using CSC markers, including ALDH$^+$, CD44^{hi}/CD24^{lo}, and mammosphere formation (Fig. 1*A* and *SI Appendix,* Table S1). Side-population analyses of CSCs were then used for validation of biological effects of miR alteration. Mature miRs were quantified in non-CSCs and CSCs by Applied Biosytems TaqMan array for almost 800 well-expressed miRs, then normalized to invariant miRs with baseline normalization and global media centering. Expression values were calculated by the 2^(-ΔΔCT) method (25). We identified 20 differentially expressed miRs that changed by ≥fivefold in common among all the nine cell lines in CSCs compared to their non-CSC cell population. Fivefold was chosen assuming this magnitude would have biological effect. miRs were queried in silico for protein synthesis factor mRNA targets, of which only miR-183 was identified, which was reduced in breast CSCs by ~13-fold (Fig. 1*B* and *SI Appendix,* Table S2). Alignment of miR-183 revealed a nearly perfect complementarity of its seed sequence to the 5′ end of the coding region of translation factor *eIF2Bδ* mRNA (Fig. 1*C*), which has not been previously identified.

miR-183 belongs to the miR-183-96-182 cluster but is independently expressed (26). It is increased in some cancers and decreased in others in association with malignancy (7, 27–29). miR-183 can regulate the EMT, and is reported to target mRNAs encoding ezrin (*VIL2*) (30), Foxo1 (31), integrin β1, isocitrate dehydrogenase 2, and ubiquitin fold modifier protein (32). miR-183 has not been previously identified as a regulator of CSCs (5).

We tested miR-183 activity by its overexpression or that of a nonsilencing scrambled miR sequence (Scr) in cancer cells.

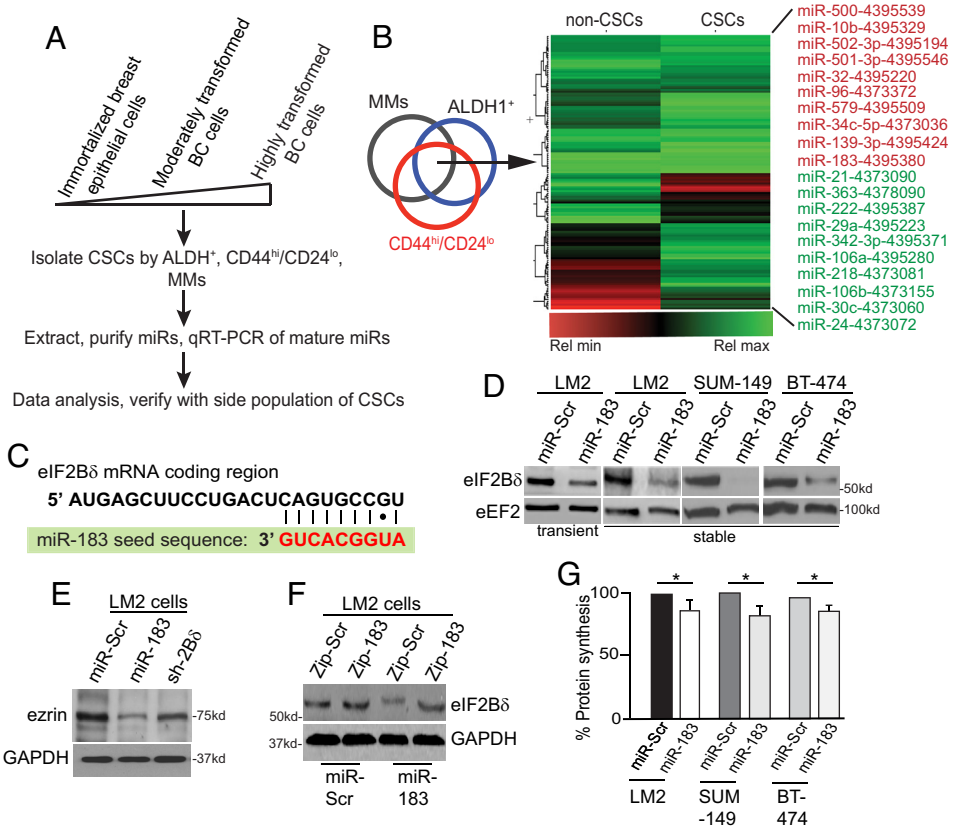

Fig. 1. Overexpression of miR-183 down-regulates eIF2Bδ protein. (*A*) Scheme for identification of miRs altered in expression in cancer stem cell populations from immortalized and progressively transformed breast cancer (BC) cell populations. MMs, mammospheres. (*B*) Heat map comparing the relative expression of miRs from the breast CSC population and the parental cell line. (*C*) Alignment of miR-183 seed sequence to the coding region of *eIF2Bδ* mRNA, present in each of the eIF2Bδ variants. (*D*) Representative immunoblot from cell lines expressing miR-Scr nonsilencing control or miR-183, by transient transfection or stable expression. eEF2, invariant loading control. n = 3. (*E*) Representative immunoblot of ezrin protein levels in cells expressing Dox-induced miR-Scr, miR-183, or shRNA to eIF2Bδ (sh-2Bδ). Glyceraldehyde-3-phosphate dehydrogenase (GAPDH), invariant loading control. n = 3. (*F*) Representative immunoblot of eIF2Bδ and GAPDH control protein levels in cells expressing a scrambled sequence (Zip-Scr) or antagomir to miR-183 (Zip-183) in cells stably expressing miR-Scr or miR-183. n = 3. (*G*) Protein synthesis rate in cells expressing miR-Scr or miR-183. *$P < 0.05$, ± SEM by two-tailed unpaired *t* test. n = 3.

Transient, constitutive, or doxycycline (Dox)-inducible expression of miR-183 by stably transduced lentivirus vectors, or a stably integrated and constitutively expressed short hairpin RNA (shRNA) specific to the *eIF2Bδ* mRNA (sh-2Bδ), strongly reduced protein levels of eIF2Bδ in all cell lines tested and moderately reduced ezrin levels (Fig. 1 *D* and *E*). Expression of an antagomir RNA to miR-183 increased eIF2Bδ protein levels in miR-183 overexpressing cells (Fig. 1*F*). Overexpression of miR-183 and reduced levels of eIF2Bδ resulted in a moderate (~15%) overall reduction in protein synthesis activity (Fig. 1*G*), which would be consistent with reduced eIF2B GEF activity.

Silencing eIF2Bδ by miR-183 Expression Strongly Reduces the Breast CSC Population. Since miR-183 is poorly expressed in breast CSCs, we asked whether enforced expression of miR-183 impairs the maintenance and function of CSCs. CSCs were quantified by Hoechst 33342 staining of a side population, $ALDH^+$ and $CD44^{hi}/CD24^{lo}$ markers from BC cell lines constitutively overexpressing miR-Scr or miR-183. LM2 cells used in this study were quantified by side population rather than by CSC marker $CD44^{hi}/CD24^{lo}$ which 99% of the non-CSC cells also express, and because these cells also express green fluorescent protein (GFP) tat interferes with the ALDH activity assay(33). Overexpression of miR-183 strongly reduced CSCs by biomarker and functional analysis in all cell lines tested (Fig. 2 *A–C* and *SI Appendix*, Fig. S1 *A–C*). Enforced expression of miR-183 also greatly reduced the ability of LM2 and SUM-149 cells to produce mammospheres, a test of CSC functional activity (Fig. 2*D* and *SI Appendix*, Fig. S1*D*). To examine whether reduced miR-183 expression increased eIF2Bδ levels in CSCs, SUM-149 CSCs were isolated by facilitated activated cell sorting (FACS), gating on the $ALDH^+$ population. eIF2Bδ protein was increased ~threefold in CSCs compared to non-CSCs, without changes in levels of the other eIF2B components (Fig. 2*E*). Low expression of miR-183 is, therefore, associated with increased levels of CSCs and increased expression of eIF2Bδ.

The reduction in CSCs resulting from enforced expression of miR-183 was validated by the expression of sh-2Bδ (Fig. 2*F*), which also significantly reduced CSCs (Fig. 2 *G* and *H*). eIF2Bδ silencing reduced protein synthesis activity in LM2 and SUM-149 cells by 15 to 20% (Fig. 2*I*), similar to miR-183. miR-183 and sh-2Bδ also greatly reduced Matrigel invasion activity of LM2 and SUM-149 cells (Fig. 2*J*), with no significant change in cell proliferation rates (*SI Appendix*, Fig. S1*E*). Thus, silencing eIF2Bδ specifically by shRNA or with miR-183 expression depletes CSCs and moderately reduces overall protein synthesis and cell in vitro invasion activity. Many of the cell physiological effects of miR-183

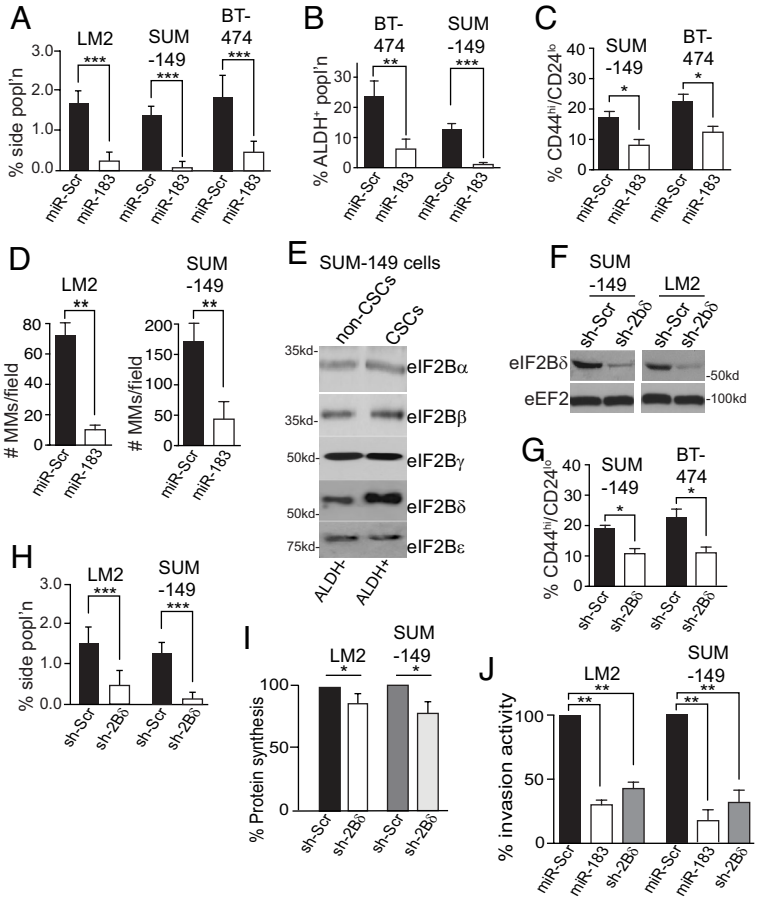

Fig. 2. Reduction in eIF2Bδ decreases breast CSCs and breast cancer cell invasion activity. (*A*) Percent side population of cells stably expressing miR-Scr or miR-183 RNAs. (*B*) Percent $ALDH^+$ in cells stably expressing miR-Scr or miR-183 RNAs. (*C*) Percent $CD44^{hi}/CD24^{lo}$ of cells stably expressing miR-Scr or miR-183 RNAs. (*D*) Number of mammospheres per field from cells stably expressing miR-Scr or miR-183 RNAs. Spheres scored contained ≥30 cells, five visual fields scored at 5× magnification chosen at random. MMs, mammopheres. (*E*) Representative immunoblot of eIF2B subunit proteins in SUM-149 cells isolated by $ALDH^+$ FACS into non-CSC and CSC populations. Equal protein amounts used. n = 3. (*F*) Representative immunoblot of eIF2Bδ in cells expressing sh-Scr or sh-2Bδ silencing RNAs. eEF2, invariant loading control. Equal protein amounts used. n = 3. (*G*) Percent $CD44^{hi}/CD24^{lo}$ cells stably expressing sh-Scr or sh-2Bδ silencing RNAs. n = 3. (*H*) Percent side population of cells stably expressing sh-Scr or sh-2Bδ silencing RNAs. (*I*) Protein synthesis activity of cells, expressing sh-Scr or sh-2Bδ silencing RNAs, measured by [^{35}S]-methionine metabolic labeling, normalized to nonsilencing controls. (*J*) Percent Matrigel transwell invasion activity of cells stably expressing miR-Scr, miR-183, or sh-2Bδ. n = 3. **P* < 0.05, ***P* < 0.01, ****P* < 0.001 ± SEM by two-tailed unpaired *t* test. n = 3.

expression therefore result in part from its regulation of eIF2Bδ levels.

Increased Expression of eIF2Bδ Expands the Breast CSC Population. We asked whether ectopic overexpression of eIF2Bδ increases the CSC population. eIF2Bδ is thought to be expressed as two and possibly three highly related variants (V) known as eIF2BδV1 (543 amino acids, major form), an N-terminal truncation V2 (523 amino acids, poorly expressed), and possibly V3 (522 amino acids, possibly minor form) that appear to be functionally identical (34, 35). We stably transfected SUM149 and LM2 cells with a plasmid expressing Flag-tagged eIF2BδV1 which was overexpressed threefold-to-fourfold compared to nonsilencing control LM2 cells (*SI Appendix,* Fig. S2*A*).

Expression of eIF2BδV1 did not measurably change protein synthesis activity in LM2 cells (*SI Appendix,* Fig. S2*B*). While expression of miR-183 or sh-2Bδ significantly reduced levels of CSCs, expression of eIF2BδV1 increased CSCs by ~twofold (*SI Appendix,* Fig. S2*C*). Overexpression of eIF2BδV1 in LM2 cells increased cell invasion activity by 50% (*SI Appendix,* Fig. S2*D*). Moreover, overexpression of eIF2BδV1 could overcome endogenous eIF2Bδ silencing by miR-183 or sh-2Bδ and significantly restore invasion activity (*SI Appendix,* Fig. S2*D*) as well as generate multi-passage mammospheres in SUM-149 cells (*SI Appendix,* Fig. S2 *E* and *F*). While miR-183 overexpression reduced SUM-149 cell mammosphere seeding by sixfold, eIF2BδV1 overexpression increased it by twofold. Increased eIF2Bδ protein levels therefore increase and maintain the breast CSC population, and BC cell invasion activity.

eIF2Bδ Expression Increases the Breast Tumor CSC Population and Promotes BC Cell Metastasis. To assess the effect of miR-183 and eIF2Bδ expression levels in regulating BC metastasis, we generated xenograft animal models using LM2 cells constitutively expressing miR-183 or control miR-Scr. LM2 cells are highly metastatic to lungs and other sites and express luciferase, enabling bioluminescence imaging (33). Cells were injected into the flank of NOD/SCID/γ immune-deficient mice and primary tumor growth was quantified. With reduction of eIF2Bδ expression in tumor cells, there was a modest but statistically significant reduction in LM2 primary tumor growth by miR-183 overexpression (Fig. 3 *A* and *B*). However, enforced miR-183 expression strongly impaired metastasis of LM2 cells to lung (Fig. 3*C*), quantified as eightfold by bioluminescence imaging (Fig. 3*D*).

We therefore asked whether overexpression of eIF2Bδ increases BC cell metastatic activity. LM2 cells were developed that expressed Dox-inducible miR-183, miR-Scr, or eIF2BδV1. NOD/SCID/γ mice were injected in the flank with equal numbers of cells, tumors

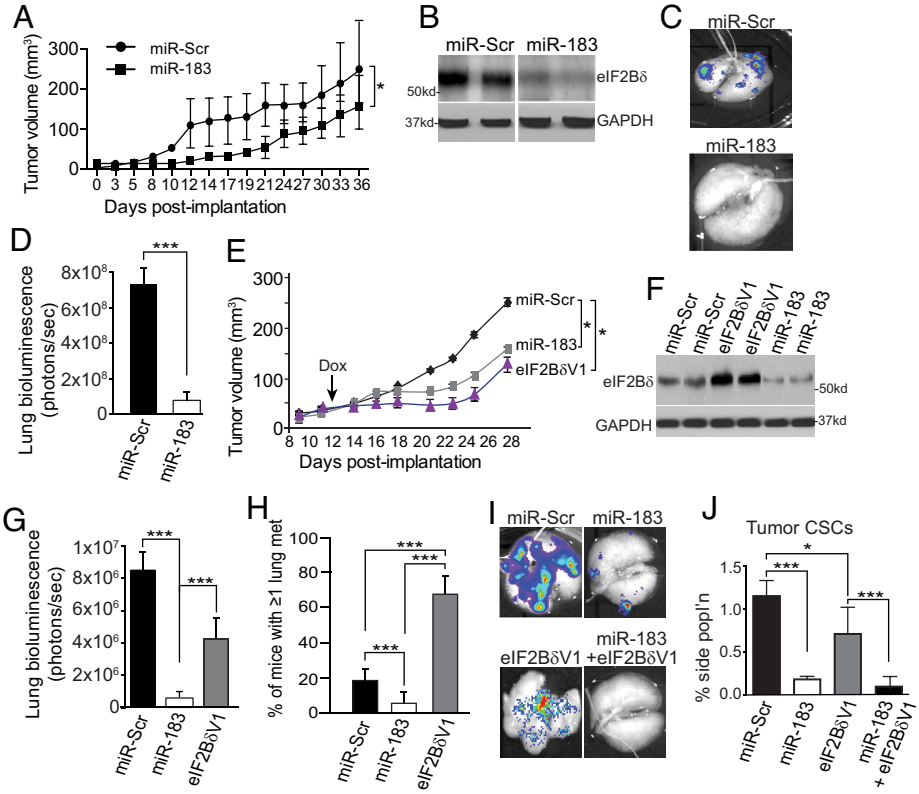

Fig. 3. eIF2Bδ is required for tumor metastasis and maintenance of the tumor CSC population. (*A*) LM2 primary tumor volume sizes in NOD/SCID/γ mice injected in the flank, constitutively expressing miR-Scr or miR-183, measured three times weekly by a precision caliper. n = 2, 10 mice per group. (*B*) Representative immunoblot of eIF2Bδ from two mice per group in primary tumors from (*A*) at d36. (*C*) Bioluminescent image of luciferase in excised lungs of mice from (*A*) at d36. Representative of 10 animals per group. (*D*) Quantification of metastatic burden in lungs of mice from (*A*) at d36. Total luciferase fluorescent flux quantified as photons (ps)/s in excised lungs, representative of total lung tumor burden. 10 mice per group, n = 2. (*E*) LM2 primary tumor volume sizes in NOD/SCID/γ mice injected in the flank, expressing Dox-inducible miR-Scr, miR-183, or eIF2BδV1, induced at d12 by addition of Dox to drinking water. Tumors measured three times weekly by a precision caliper. n = 2, 10 mice per group. (*F*) Representative immunoblot of eIF2Bδ from two mice per group in tumors from (*E*). (*G*) Quantification of metastatic burden in lungs of mice from (*E*) at d28. Total luciferase fluorescent flux quantified as photons (ps)/s in excised lungs. 10 mice per group, n = 2. (*H*) Quantification of number of mice with at least one metastasis per lung, from mice in (*E*) at d28, 10 mice per group, n = 2. (*I*) Bioluminescent images of luciferase activity in excised lungs from mice from d28 tumors expressing Dox-inducible miR-Scr, miR-183, eIF2BδV1 −/+miR-183. Representative of 10 mice per group. (*J*) Quantification of LM2 cell primary tumor side population from animals as shown in (*I*). n = 2, 10 mice per group. Animal tumor volume studies: $^{*}P < 0.05$ ± SEM, two-way unpaired ANOVA test with Dunnett's post-ANOVA test determination. All other studies, $^{*}P < 0.05$, $^{***}P < 0.001$ ± SEM by two-tailed unpaired *t* test from three independent trials unless stated.

were grown, and then Dox induction was initiated at d12. Expression of miR-183 reduced primary tumor growth rates (Fig. 3*E*), as found for constitutive miR-183 expression, and eIF2Bδ protein levels throughout the study (Fig. 3*F*). Induced silencing also strongly reduced lung metastatic burden (12-fold, Fig. 3*G*) and reduced the number of mice with one or more lung metastases of any size by 75% (Fig. 3*H*). Surprisingly, induced overexpression of eIF2BδV1 also reduced primary tumor growth rates, and reduced by half metastasis to lung, as quantified by bioluminescence imaging (Fig. 3*G*). However, further analysis showed that overexpression of eIF2BδV1 increased the number of mice with ≥1 metastatic lesion in lung by more than threefold (Fig. 3*H*). Accordingly, lung imaging showed that whereas control mice typically had only several very large and therefore highly bioluminescent lung metastases, eIF2BδV1 overexpression in primary tumors gave rise to numerous small and therefore weakly bioluminescent lung metastases (Fig. 3*I*). Coexpression of eIF-2BδV1 and miR-183 blocked metastasis, suggesting that the more rapid seeding of metastasis by primary tumors was due to overexpression of eIF2Bδ. Analysis of primary tumor CSC numbers was consistent with this suggestion, demonstrating fewer CSCs in primary tumors with eIF2BδV1 overexpression (Fig. 3*J*). That primary tumor CSCs were dependent on eIF2Bδ expression was shown by cooverexpressing miR-183, which strongly reduced both primary tumor CSC numbers and lung metastasis (Fig. 3 *I* and *J*).

Increased Expression of eIF2Bδ in BC Cells Suppresses the ISR. We first determined whether overexpressed eIF2Bδ protein is incorporated into the eIF2B decameric complex. eIF2B decamers were isolated from LM2 cells stably transfected with control miR-Scr or eIF2BδV1 mRNA-expressing plasmids. Equal protein amounts of LM2 cell lysates (Fig. 4 *A*, *Left*) were resolved by high salt, 5 to 20% sucrose gradient sedimentation in an SW55 rotor to dissociate eIF2B from eIF2 (36). Thirteen equal volume fractions were collected and subjected to SDS-PAGE electrophoresis and immunoblot analysis. When isolated in this manner, eIF2B decamers sediment in sucrose gradient fractions 6 to 8 (36). Pooled fractions 6 to 8 from LM2 cells overexpressing eIF2BδV1-Flag contained similar levels of the five eIF2B proteins, including eIF2Bδ, compared to vector controls (Fig. 4 *A*, *Right*). The bottom panel shows the Flag-tagged V1 and endogenous forms of eIF2Bδ, that coisolated with eIF2B complexes. Increased expression of eIF2Bδ is not associated with significantly elevated levels of eIF2B decamers.

We therefore determined whether overexpression of eIF2Bδ results in eIF2Bδ protein that is not associated with the eIF2B complex. Because eIF2Bδ and α interact to form a stable tetramer $(eIF2B\alpha\delta)_2$ (21), levels of tetramer formation can indicate whether there is eIF2Bδ not incorporated into the eIF2B complex. Immunoprecipitation of eIF2Bδ from equal amounts of LM2 cell cytoplasmic lysates stably transfected with

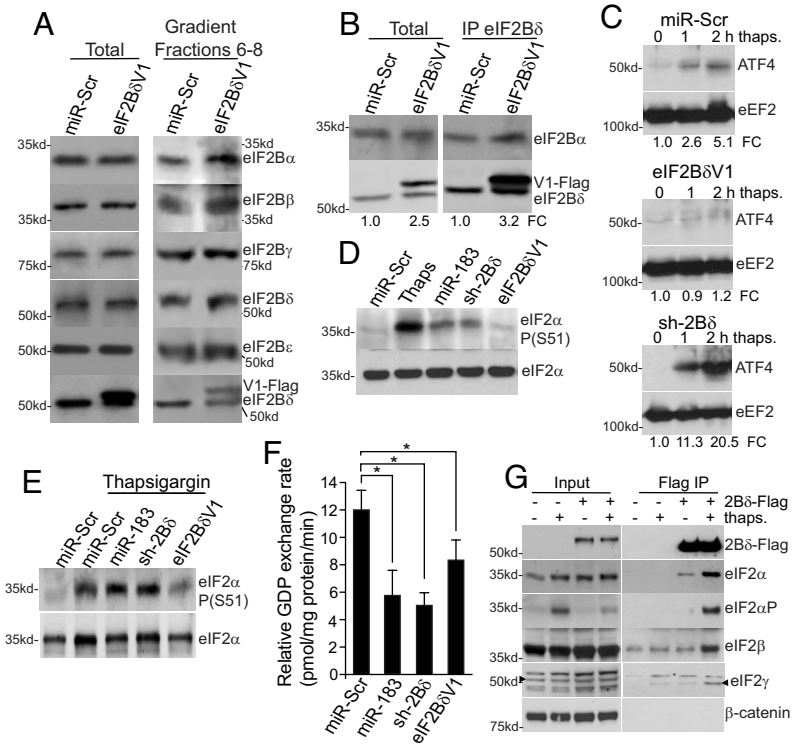

Fig. 4. Increased expression of eIF2Bδ represses the ISR in breast cancer cells. (*A*) Representative immunoblots of eIF2B proteins isolated from LM2 cells stably expressing miR-Scr or eIF2BδV1 (Flag-tagged). Total lysates (*Left*); eIF2B decamer containing fractions 6 to 8 of 5 to 20% high salt sucrose gradient sedimentation (*Right*). (*B*) LM2 cells stably expressing miR-Scr or eIF2BδV1 (Flag-tagged) were immunoprecipitated for eIF2Bδ and immunoblotted for eIF2Bα or δ. Endogenous and flag-tagged eIF2BδV1 were slightly electrophoretically separated. Total and immunoprecipitated proteins shown. (*C*) LM2 cells stably expressing miR-Scr, sh2Bδ or eIF2BδV1 treated with 30 μM thapsigargin for 2 h, equal protein amounts subjected to immunoblot for ATF4 or eEF2 invariant control. n = 3. FC, fold change normalized to eEF2. (*D*) Representative immunoblot of eIF2α Ser-51 phosphorylation in LM2 cells expressing miR-Scr, miR-183, sh-2Bδ or eIF2BδV1. Control cells treated for 2 h with 30 μM thapsigargin. Equal protein amounts immunoblotted. n = 2. (*E*) Representative immunoblot of eIF2α Ser-51 phosphorylation in LM2 cells expressing miR-Scr, miR-183, sh-2Bδ or eIF2BδV1 treated for 2 h with 30 μM thapsigargin. Equal protein amounts immunoblotted. n = 2. (*F*) Guanine nucleotide exchange activity of LM2 cells expressing miR-Scr, miR-183, sh-2Bd, or eIF2BδV1. (*G*) Immunoprecipitation of eIF2 and P-eIF2 (α-Ser51) by eIF2Bδ. Representative immunoblots of three independent studies of eIF2–eIF2BδV1 (2Bδ-Flag) interaction blotted for all the three eIF2 proteins, −/+ thapsigargin induction of the ISR. Treatment and transfections as in panel *C*. Data shown for *F* are ±SEM of three independent experiments carried out in triplicate. **P* < 0.05, ***P* < 0.01 ± SEM by two-tailed unpaired *t* test, n = 3.

control miR-Scr or eIF2BδV1-Flag expressing plasmids, showed that despite threefold-to-fourfold increased expression of eIF2BδV1-Flag, there was not a large increase in the amount of coimmunoprecipitated eIF2Bα (Fig. 4*B*). Thus, with a threefold-to-fourfold increased expression of eIF2Bδ as found in CSCs, there is a pool of unassociated eIF2Bδ.

Malignant cancer cells utilize the ISR response to control ER stress and restore ER proteostasis, enabling survival to stresses such as hypoxia and nutrient deprivation, in part by conferring tumor cell dormancy during stress (37). CSCs, however, must be able to withstand physiological stresses while remaining metabolically active and maintaining some level of protein synthesis to enable migration, invasion, and metastasis (2). Neither silencing of endogenous eIF2Bδ nor overexpression of eIF2BδV1 in unstressed LM2 cells had any statistically significant effect on ISR activation markers *ATF4* and *CHOP* mRNA levels, or ATF4 protein levels (*SI Appendix,* Fig. S3*A*). However, treatment of LM2 cells with 30 μM thapsigargin to induce an ISR increased ATF4 protein expression by >fivefold within 2 h in control cells, and >20-fold with eIF2Bδ silencing, but was suppressed by increased expression of eIF2BδV1 (Fig. 4*C*), with only small changes in *ATF4* mRNA levels (*SI Appendix,* Fig. S3*B*). Similarly, *CHOP* mRNA levels, indicative of ISR activation, were increased 12-fold in eIF2Bδ-silenced cells by 2 h of thapsigargin treatment, whereas overexpression of eIF2Bδ, like control sh-SCR, had no effect on CHOP mRNA levels (*SI Appendix,* Fig. S3*C*). Increased expression of eIF2Bδ therefore functions as a negative regulator of the ISR in BC cells.

eIF2α Ser51 phosphorylation is a hallmark of ISR activation and is essential for translation of ATF4. In unstressed LM2 cells expressing miR-183 or sh-2Bδ, there was a higher level of eIF2α Ser51 phosphorylation, not seen with eIF2BδV1 overexpression (Fig. 4*D*), but much lower than the thapsigargin control. However, induction of eIF2α phosphorylation by thapsigargin was partially suppressed by increased expression of eIF2BδV1, whereas eIF2Bδ silencing did not block phosphorylation (Fig. 4*E*). Thus, increased expression of eIF2Bδ suppresses the ISR in BC cells, including phosphorylation of eIF2α.

We asked whether the expression level of eIF2Bδ alters eIF2B GEF activity. LM2 cells overexpressing miR-Scr, miR-183, sh-2Bδ or eIF2BδV1 were analyzed for eIF2B GEF activity in cell-free extracts that have been shown to respond to alterations in eIF2B activity or proteins (38, 39) (Fig. 4*F*). Reduced expression of eIF2Bδ by either miR-183 or sh-2Bδ silencing reduced GEF activity by 50 to 60%, as expected. Surprisingly, GEF activity was reduced ~20% by eIF2BδV1 overexpression, although protein synthesis activity was maintained under these conditions (*SI Appendix,* Fig. S2*B*), suggesting that overexpressed eIF2Bδ preserves protein synthesis, blocks induction of the ISR, and partially blocks eIF2α phosphorylation, but with some limitation to eIF2B guanine exchange activity.

The structural determination and biochemical understanding of the eIF2B complex has identified eIF2Bδ as part of the regulatory core of eIF2B (19–21, 40–42). eIF2Bδ interacts with eIF2Bα, which joins the two pentamers of eIF2B together, creating a stable decameric complex. Moreover, eIF2Bδ is critical for eIF2B interaction with, and inhibition by, phosphorylated eIF2. Unphosphorylated eIF2 interacts with eIF2B through its eIF2γ subunit, which binds a catalytic pocket formed by eIF2Bβ and eIF2Bδ subunits (43, 44). However, phosphorylated eIF2 interacts with eIF2B by binding between eIF2Bα and eIF2Bδ subunits (43–46), which blocks GTP exchange activity (43). The structural understanding of eIF2B provides a framework to now investigate the mechanism by which increased expression of eIF2Bδ increases the ability of cancer cells and particularly metastatic CSCs, which are under strong physiological stress (47, 48), to resist inhibition of eIF2B and eIF2α phosphorylation by the ISR, and attenuation of the ISR as well.

We therefore asked whether overexpressed eIF2Bδ, which we have shown to be not part of the eIF2B complex, interacts with eIF2 as a means to prevent eIF2α-P inhibition of eIF2B. LM2 cells were transiently transfected with an eIF2BδV1-Flag expression plasmid, without and with 2 h treatment with thapsigargin to stimulate eIF2α Ser51 phosphorylation. eIF2BδV1 was immunoprecipitated and immunoblotted (Fig. 4*G*). Overexpressed eIF2Bδ interacted strongly with Ser-51 phosphorylated eIF2α but only weakly with the nonphosphorylated protein, and as part of the eIF2 complex, shown by the presence of eIF2β and γ proteins as well. These data indicate that unassociated eIF2Bδ likely intercepts eIF2α-P, reducing inhibition of eIF2B.

Our data indicate that increased levels of eIF2Bδ as a result of reduced miR-183 expression are unlikely to increase eIF2B complex levels, but rather, result in increased levels of unassociated eIF2Bδ. eIF2αP binds eIF2B between the α and δ subunits. eIF2Bδ not associated with eIF2B binds preferentially to eIF2αP, possibly blocking its interaction with eIF2B decamers, which likely blunts propagation of the ISR. Interestingly, a study in yeast using recombinant eIF2α protein independent of the eIF2 trimer complex did not detect stable interaction with free eIF2Bδ protein, regardless of eIF2α Ser-51 phosphorylation (49). Either yeast and mammalian eIF2B–eIF2α interactions differ, or more likely, eIF2α must be in the eIF2 complex to interact with eIF2Bδ that is not associated with the eIF2B complex, as in our study. Future studies need to determine if this is the mechanism by which increased levels of eIF2Bδ blunt amplification of the ISR.

ISRIB is a small-molecule inhibitor that blocks the ISR by targeting eIF2Bδ, altering the structural interaction between the α and δ subunits in eIF2B pentamers (50, 51), which impairs interaction with eIF2αP (52). Therefore, ISRIB and overexpressed eIF2Bδ have different mechanisms of action. In fact, while both ISRIB and overexpressed eIF2Bδ suppress the ISR, in experimental animal tumor models, treatment with ISRIB significantly inhibited primary tumor growth and metastasis (22, 23), whereas overexpression of eIF2Bδ had only a slight impact on tumor growth, but strongly increased metastasis. Unlike the overexpression of eIF2Bδ, ISRIB does not block eIF2α phosphorylation, but increases eIF2B GEF activity (36, 53), whereas increased levels of eIF2Bδ modestly reduced eIF2B GEF activity and reduced but did not abolish eIF2α phosphorylation. Our studies suggest that overexpressed eIF2Bδ is largely not in a complex with eIF2B and interferes with eIF2αP–eIF2B engagement. However, it remains to be determined whether increased expression of eIF2Bδ promotes the generation of eIF2B subcomplexes, possibly increasing the levels of catalytic γ/ε catalytic core subcomplexes that can carry out reduced GEF activity but are insensitive to the ISR (19, 21, 45). Either or both mechanisms could be in effect, and both can explain how overexpression of eIF2Bδ can act both upstream and downstream of eIF2B, reduce eIF2α phosphorylation, block the ISR, and maintain some level of eIF2B activity.

Materials and Methods

Mouse Tumor Studies. All studies were approved by the NYU Grossman School of Medicine's Institutional Animal Care and Use Committee (IACUC) and conducted in accordance with IACUC guidelines. Female 6-8-wk-old NOD/SCIDγ immunodeficient mice were used for human cell line tumor studies (Jackson Laboratories, Bar Harbor, ME). Mice were injected subcutaneously (s.c.) in the 4th mammary fat pad with 5×10^5 BC cells in a total volume of 200 μL with CORNING Matrigel matrix (Corning). The mice were randomized to treatment

groups to receive placebo or Dox in their drinking water to induce miR expression. Dox was added to drinking water at 100 mg/mL in 50 mg/mL sucrose. Control studies used only 50 mg/mL sucrose in drinking water. To obtain tumor growth curves, perpendicular length measurements and tumor volumes were calculated using the formula ($\pi/6 \times L \times W^2$). Mouse tumor volumes were scored throughout the trial by a precision caliper as indicated in figure legends. The mice were killed by first anesthetizing with isofluorane, followed by cervical dislocation. All experiments were conducted according to the university's IUCAC protocol. Tumors and lungs were excised for analysis at the times indicated in figure legends.

Bioluminescent Imaging of Tumors. Tumor growth studies used bioluminescent imaging (IVIS Lumina III). Imaging was carried out until flux over the defined region of interest (ROI) of the mouse abdomen achieved approximately 10^8 photons/second. To quantify tumor luciferase expression, animals were injected IP with 200 μL luciferin (diluted in phosphate buffered saline (PBS) per manufacturer's instructions). The animals were imaged in groups of 3. Images were analyzed using Living Image software. The ROI was defined using an ellipse surrounding the mouse abdomen. Flux was calculated within the ROI for each mouse and averaged across all mice within each treatment group. Average flux was compared across groups over time and normalized to baseline flux levels prior to initiation of Dox or control treatment. Mice were killed if they became terminally moribund. Lungs were excised and imaged ex vivo immediately after surgical excision, by inflation with 1× cold PBS prior to imaging.

miRNA Extraction, TaqMan Mature microRNA qPCR Assay Quantification, and Analysis. miRNAs were extracted from cells using the miRvana miRNA Isolation kit. RNA concentration and purity were quantified using a NanoDrop Spectrophotometer (Thermo Fisher Scientific). The TaqMan Advanced MicroRNA cDNA Synthesis Kit and miRNA Assay (Applied Biosystems, Foster City, CA) were used to quantify mature miRs using RT-PCR in an ABI 7500 Real-Time PCR system (Applied Biosystems) in a 96-well format. This system uses a stem-loop primer to amplify mature miRs for almost 800 well-expressed miRs. All assays were performed in triplicate according to manufacturer's instructions. First-strand cDNA was synthesized from 100 ng total RNA using the High-Capacity cDNA Reverse Transcription Kit (Thermo Fisher Scientific). qRT-PCR (qPCR) analysis was performed using 500 ng cDNA, 2 μM primers (*SI Appendix*, Resources and Antibodies Table), and Maxima SYBR Green qPCR Master Mix (2X) (Bio-Rad Laboratories). The relative expression level of each miR was normalized to that of invariant miR-16 and U6 RNAs with baseline normalization and global median centering. Expression values were calculated utilizing the 2^(−ΔΔ CT) method (25).

eIF2B Protein miR and shRNA Silencing. Lentiviruses were produced by transient transfection of human embryonic kidney 293FT cells with individual lentiviral vectors containing the pLKO-Tet-On or pLKO constitutive vectors with packaging plasmids pMD2G and psPAX2 (Addgene, Cambridge, MA, USA) using Lipofectamine 2000 (Promega, Madison, WI, USA). Supernatants containing viral particles were collected 48 h posttransfection and filtered through 0.45 μm filters and the viral particles were concentrated using the PEG-itTM Virus Precipitation Solution Kit (System Biosciences, Mountain View, CA, USA). Cloning of the shRNA cassette sequences for eIF2Bδ and nonsilencing sequence control Nsi (5′-AATTCTCCGAACGTGTCACGT-3′) was previously described (34). Cells were infected with viral particles, selected with puromycin (1 μg/mL). The lentiviral vectors used for miR-183, miR-Scr, and sh-eIF2Bδ contain a constitutively expressed transcript encoding the puromycin resistance gene. Cells were treated with 0.1 to 2 μg/mL Dox and FACs isolated gating on GFP for isolation.

Flow Cytometry of CD44^{hi}/24^{lo} Population. For cell sorting, typically 2×10^6 cells were incubated with anti-human CD24 and anti-human CD44 for 30 min on ice. After the incubation, cells were washed 2X with a solution of 2% fetal bovine serum (FBS)/PBS and resuspended at 1×10^6 cells/mL in 2% FBS/PBS. The cells were sorted using FACSARIA II cell sorter. For cell analysis, 2×10^5 cells were used for the labeling reaction and analyzed using the LSR II UV analyzer. Antibody concentrations were titrated and optimized before sorts and analyses.

Side-Population Flow Cytometry. 500,000 cells were stained with bisBenzimide H 33342 trihydrochloride, and half of the sample was cotreated with 50 μM verapamil hydrochloride. Incubations were carried out at 37 °C for 30 min after which cells were washed 2X with ice-cold 2% FBS/PBS, resuspended in ice-cold 2% FBS/PBS, and analyzed using an LSR II UV analyzer.

Tumor Lysis and Extract Preparation. Tumors were homogenized using a pellet pestle in lysis buffer which consisted of 1% Triton X-100, 1% sodium deoxycholate, 0.1% SDS, 150 mM NaCl, 50 mM Tris, pH 7.4, 2 mM Na_3VO_4, 25 mM β-glycerophosphate, 15 mM NaF, and complete protease inhibitor mix (Roche). Protein concentrations in the lysates of cells lysed in RIPA lysis buffer were determined using a DC protein assay kit (Bio-Rad).

Sucrose Density Gradient Analysis of eIF2B Complexes. Sucrose gradient studies were conducted as previously described (36). Briefly, LM2 cells were collected and washed with ice-cold PBS and then lysed in lysis buffer (50 mM Tris pH = 7.5, 400 mM KCl, 4 mM $Mg(OAc)_2$, 0.5% Triton X-100, and protease inhibitors). Lysates were clarified and ribosomes were removed by pelleting under high-speed centrifugation at 100,000 × g for 30 min at 4 °C. Supernatants were layered on the top of 5 to 20% sucrose gradients and centrifuged for 14 h at 40,000 rpm at 4 °C using an SW55 rotor. Equal fractions were collected from gradients, proteins were precipitated with chloroform-methanol and resolved by SDS-polyacrylamide gel electrophoresis.

Ethical Compliance. All experiments involving live animals were carried out at New York University Grossman School of Medicine in full compliance with ethical regulations approved by the IACUC Committee. The protocol for collection of human BC tissue specimens was approved by the New York University Langone Health/Grossman School of Medicine's Institutional Review Board and obtained from deidentified and consented individuals in compliance with all ethical regulations.

Statistical Analysis. Statistical significance was assessed by two-tailed *t* test for unpaired experimental values or one-way or two-way ANOVA tests with Dunnett's post-ANOVA test determination for analysis of repeated measures as indicated in figure legends. Data were expressed as indicated in figure legends as means with SEM, and when appropriate corrected for sample sizes using Bonferroni corrections to adjust alpha values. Significance difference was defined as $P < 0.05$. Statistical analyses were performed using GraphPad 8 or 9 software (GraphPad Software, Inc., San Diego, CA, USA).

Data, Materials, and Software Availability. All study data are included in the article and/or *SI Appendix*.

ACKNOWLEDGMENTS. We thank B. Dinardo, A. Gadi, and K. Granados Blanco (NYU) for their technical help with studies, and S. Kimball (Penn State University) for help with the eIF2B GEF studies. NYU Medical Center core services were supported by National Cancer Institute (NCI) P30CA016087 and National Center for Advancing translational Science UL1TR00038; this work was supported by National Institute of General Medicine 5T32 GM066704 and a Howard Hughes Medical Institute Gilliam Fellowship (P.A.G.); T32 CA9161-41 (B.A.W.); and Breast Cancer Research Foundation BCRF-21-146, NCI R01CA178509, and R01CA248397 (R.J.S.).

Author affiliations: [a]Department of Microbiology, New York University Grossman School of Medicine, New York, NY 10016; and [b]New York University Perlmutter Cancer Center, New York University Grossman School of Medicine, New York, NY 10016

1. D. R. Pattabiraman, R. A. Weinberg, Tackling the cancer stem cells–what challenges do they pose? *Nat. Rev. Drug Discov.* **13**, 497–512 (2014).
2. C. Peitzsch, A. Tyutyunnykova, K. Pantel, A. Dubrovska, Cancer stem cells: The root of tumor recurrence and metastases. *Semin. Cancer Biol.* **44**, 10–24 (2017).
3. M. Al-Hajj, M. S. Wicha, A. Benito-Hernandez, S. J. Morrison, M. F. Clarke, Prospective identification of tumorigenic breast cancer cells. *Proc. Natl. Acad. Sci. U.S.A.* **100**, 3983–3988 (2003).
4. J. Dittmer, Breast cancer stem cells: Features, key drivers and treatment options. *Semin. Cancer Biol.* **53**, 59–74 (2018).
5. T. Niu, W. Zhang, W. Xiao, MicroRNA regulation of cancer stem cells in the pathogenesis of breast cancer. *Cancer Cell Int.* **21**, 31 (2021).
6. G. Pan, Y. Liu, L. Shang, F. Zhou, S. Yang, EMT-associated microRNAs and their roles in cancer stemness and drug resistance. *Cancer Commun. (Lond).* **41**, 199–217 (2021).
7. D. Cao *et al.*, MicroRNA-183 in cancer progression. *J. Cancer* **11**, 1315–1324 (2020).
8. S. Volinia *et al.*, Pluripotent stem cell miRNAs and metastasis in invasive breast cancer. *J. Natl. Cancer Inst.* **106**, dju324 (2014).
9. H. E. Gee *et al.*, MicroRNA-10b and breast cancer metastasis. *Nature* **455**, E8–E9 (2008).

10. S. J. Song *et al.*, MicroRNA-antagonism regulates breast cancer stemness and metastasis via TET-family-dependent chromatin remodeling. *Cell* **154**, 311–324 (2013).
11. L. Y. Chen *et al.*, The circular RNA circ-ERBIN promotes growth and metastasis of colorectal cancer by miR-125a-5p and miR-138-5p/4EBP-1 mediated cap-independent HIF-1alpha translation. *Mol. Cancer* **19**, 164 (2020).
12. Y. Zhou, Y. Wang, L. Wang, J. Zhang, X. Liu, Decreased microRNA-768-3p expression indicates a poor prognosis in patients with breast cancer and promotes breast cancer cell viability, migration and invasion. *Oncol. Lett.* **22**, 579 (2021).
13. Y. Zhang, Q. Tie, Z. Bao, Z. Shao, L. Zhang, Inhibition of miR-15a-5p promotes the chemoresistance to pirarubicin in hepatocellular carcinoma via targeting eIF4E. *Comput. Math. Methods Med.* **2021**, 6468405 (2021).
14. R. Liang *et al.*, H19X-encoded miR-322(424)/miR-503 regulates muscle mass by targeting translation initiation factors. *J. Cachexia Sarcopenia Muscle* **12**, 2174–2186 (2021).
15. X. Pan *et al.*, Downregulation of eIF4G by microRNA-503 enhances drug sensitivity of MCF-7/ADR cells through suppressing the expression of ABC transport proteins. *Oncol. Lett.* **13**, 4785–4793 (2017).
16. W. C. Merrick, G. D. Pavitt, Protein synthesis initiation in Eukaryotic cells. *Cold Spring Harb. Perspect. Biol.* **10**, a033092 (2018).
17. R. C. Wek, Role of eIF2alpha kinases in translational control and adaptation to cellular stress. *Cold Spring Harb. Perspect. Biol.* **10**, a032870 (2018).
18. A. Marintchev, T. Ito, eIF2B and the integrated stress response: A structural and mechanistic view. *Biochemistry* **59**, 1299–1308 (2020).
19. Y. Gordiyenko *et al.*, eIF2B is a decameric guanine nucleotide exchange factor with a gamma2epsilon2 tetrameric core. *Nat. Commun.* **5**, 3902 (2014).
20. N. C. Wortham, M. Martinez, Y. Gordiyenko, C. V. Robinson, C. G. Proud, Analysis of the subunit organization of the eIF2B complex reveals new insights into its structure and regulation. *FASEB J.* **28**, 2225–2237 (2014).
21. B. Kuhle, N. K. Eulig, R. Ficner, Architecture of the eIF2B regulatory subcomplex and its implications for the regulation of guanine nucleotide exchange on eIF2. *Nucleic Acids Res.* **43**, 9994–10014 (2015).
22. H. G. Nguyen *et al.*, Development of a stress response therapy targeting aggressive prostate cancer. *Sci. Transl. Med.* **10**, eaar2036 (2018).
23. N. Ghaddar *et al.*, The integrated stress response is tumorigenic and constitutes a therapeutic liability in KRAS-driven lung cancer. *Nat. Commun.* **12**, 4651 (2021).
24. N. Robichaud, N. Sonenberg, D. Ruggero, R. J. Schneider, Translational control in cancer. *Cold Spring Harb. Perspect. Biol.* **11**, a032896 (2019).
25. K. J. Livak, T. D. Schmittgen, Analysis of relative gene expression data using real-time quantitative PCR and the 2(-Delta Delta C(T)) method. *Methods* **25**, 402–408 (2001).
26. M. Lagos-Quintana, R. Rauhut, J. Meyer, A. Borkhardt, T. Tuschl, New microRNAs from mouse and human. *RNA* **9**, 175–179 (2003).
27. A. J. Lowery, N. Miller, R. M. Dwyer, M. J. Kerin, Dysregulated miR-183 inhibits migration in breast cancer cells. *BMC Cancer* **10**, 502 (2010).
28. L. Zhou *et al.*, MicroRNA-183 is involved in cell proliferation, survival and poor prognosis in pancreatic ductal adenocarcinoma by regulating Bmi-1. *Oncol. Rep.* **32**, 1734–1740 (2014).
29. X. L. Zhang, S. H. Pan, J. J. Yan, G. Xu, The prognostic value of microRNA-183 in human cancers: A meta-analysis. *Medicine (Baltimore)* **97**, e11213 (2018).
30. H. Yan *et al.*, Upregulation of miR-183-5p is responsible for the promotion of apoptosis and inhibition of the epithelial-mesenchymal transition, proliferation, invasion and migration of human endometrial cancer cells by downregulating Ezrin. *Int. J. Mol. Med.* **42**, 2469–2480 (2018).
31. R. Suzuki *et al.*, miR-182 and miR-183 promote cell proliferation and invasion by targeting FOXO1 in mesothelioma. *Front. Oncol.* **8**, 446 (2018).
32. S. Dambal, M. Shah, B. Mihelich, L. Nonn, The microRNA-183 cluster: The family that plays together stays together. *Nucleic Acids Res.* **43**, 7173–7188 (2015).
33. A. J. Minn *et al.*, Genes that mediate breast cancer metastasis to lung. *Nature* **436**, 518–524 (2005).
34. L. Martin, S. R. Kimball, L. B. Gardner, Regulation of the unfolded protein response by eif2Bdelta isoforms. *J. Biol. Chem.* **285**, 31944–31953 (2010).
35. R. M. Kuhn *et al.*, The UCSC genome browser database: Update 2009. *Nucleic Acids Res.* **37**, D755–D761 (2009).
36. C. Sidrauski *et al.*, Pharmacological dimerization and activation of the exchange factor eIF2B antagonizes the integrated stress response. *Elife* **4**, e07314 (2015).
37. H. Urra, E. Dufey, T. Avril, E. Chevet, C. Hetz, Endoplasmic reticulum stress and the hallmarks of cancer. *Trends Cancer* **2**, 252–262 (2016).
38. A. Fogli *et al.*, Decreased guanine nucleotide exchange factor activity in eIF2B-mutated patients. *Eur. J. Hum. Genet.* **12**, 561–566 (2004).
39. C. J. Kershaw *et al.*, GTP binding to translation factor eIF2B stimulates its guanine nucleotide exchange activity. *iScience* **24**, 103454 (2021).
40. K. Kashiwagi *et al.*, Crystal structure of eukaryotic translation initiation factor 2B. *Nature* **531**, 122–125 (2016).
41. G. D. Pavitt, K. V. Ramaiah, S. R. Kimball, A. G. Hinnebusch, eIF2 independently binds two distinct eIF2B subcomplexes that catalyze and regulate guanine-nucleotide exchange. *Genes Dev.* **12**, 514–526 (1998).
42. A. M. Bogorad *et al.*, Insights into the architecture of the eIF2Balpha/beta/delta regulatory subcomplex. *Biochemistry* **53**, 3432–3445 (2014).
43. K. Kashiwagi *et al.*, Structural basis for eIF2B inhibition in integrated stress response. *Science* **364**, 495–499 (2019).
44. L. R. Kenner *et al.*, eIF2B-catalyzed nucleotide exchange and phosphoregulation by the integrated stress response. *Science* **364**, 491–495 (2019).
45. Y. Gordiyenko, J. L. Llacer, V. Ramakrishnan, Structural basis for the inhibition of translation through eIF2alpha phosphorylation. *Nat. Commun.* **10**, 2640 (2019).
46. T. Adomavicius *et al.*, The structural basis of translational control by eIF2 phosphorylation. *Nat. Commun.* **10**, 2136 (2019).
47. E. Madden, S. E. Logue, S. J. Healy, S. Manie, A. Samali, The role of the unfolded protein response in cancer progression: From oncogenesis to chemoresistance. *Biol. Cell* **111**, 1–17 (2019).
48. S. A. Oakes, Endoplasmic reticulum stress signaling in cancer cells. *Am. J. Pathol.* **190**, 934–946 (2020).
49. T. Krishnamoorthy, G. D. Pavitt, F. Zhang, T. E. Dever, A. G. Hinnebusch, Tight binding of the phosphorylated alpha subunit of initiation factor 2 (eIF2 alpha) to the regulatory subunits of guanine nucleotide exchange factor eIF2B is required for inhibition of translation initiation. *Mol. Cell Biol.* **21**, 5018–5030 (2001).
50. J. C. Tsai *et al.*, Structure of the nucleotide exchange factor eIF2B reveals mechanism of memory-enhancing molecule. *Science* **359**, eaaq0939 (2018).
51. A. F. Zyryanova *et al.*, Binding of ISRIB reveals a regulatory site in the nucleotide exchange factor eIF2B. *Science* **359**, 1533–1536 (2018).
52. A. F. Zyryanova *et al.*, ISRIB blunts the integrated stress response by allosterically antagonising the inhibitory effect of phosphorylated eIF2 on eIF2B. *Mol. Cell* **81**, 88–103.e6 (2021).
53. Y. Sekine *et al.*, Stress responses. Mutations in a translation initiation factor identify the target of a memory-enhancing compound. *Science* **348**, 1027–1030 (2015).